FULL PAPER

20% External Quantum Efficiency in Solution-Processed Blue Thermally Activated Delayed Fluorescent Devices

*Yong Joo Cho, Byung Doo Chin, Sang Kyu Jeon, and Jun Yeob Lee**

Highly efficient solution-processed blue thermally activated delayed fluorescent (TADF) devices are developed by designing soluble blue TADF emitters. The solubility and emission color could be managed by introducing F as an electron withdrawing unit instead of CN. Two soluble blue TADF emitters are synthesized and show a high external quantum efficiency of 20.0% with a color coordinate of (0.16,0.26), and it is the best quantum efficiency reported in solution-processed TADF devices. The device performances of the solution-processed blue TADF devices are comparable to those of vacuum-processed blue TADF devices.

1. Introduction

The development of high efficiency solution-processed organic light-emitting diodes (OLEDs) has been a great challenge in the research of OLEDs because the solution process has intrinsic problems to overcome such as material incompatibility and multilayer structure formation.[1–4] Generally, OLED materials for vacuum evaporation process are not compatible with the solution process because of poor solubility and crystallization during solution-coating process. Therefore, chemical modification of the molecular structure is needed to use small molecules for vacuum process in the solution process.[3,4]

Typically, phosphorescent emitting materials have been used as the high efficiency soluble materials for solution-processed OLEDs and provided high quantum efficiency (QE) in red, green, and blue soluble OLEDs.[5–15] Modification of chemical structure of the phosphorescent emitters was successful to solubilize the phosphorescent emitters and to obtain high QE. Great progress of the QE in the solution-processed phosphorescent OLEDs has been made for the last decade using small molecules and current QE level of the phosphorescent OLEDs is above 20%.[13–15]

Soluble thermally activated delayed fluorescent (TADF) OLEDs can be considered as an alternative of the soluble phosphorescent OLEDs because of high QE of vacuum-processed TADF OLEDs.[16–20] The QE of green and blue TADF OLEDs is as high as 20%, which suggests that the TADF OLEDs have a potential as the high efficiency solution-processed OLEDs. Our group already reported that the QE of green TADF OLEDs can be improved up to 18.3% by increasing the solubility of the TADF emitters using a *t*-butyl substituent.[21] The *t*-butyl substitution has been widely used as an approach to increase the solubility of organic materials and was successful in the design of soluble green TADF emitters. However, the *t*-butyl modification is not appropriate in the design of blue TADF emitters because of red shift of emission color due to strong electron donating character of the *t*-butyl modified carbazole unit. Therefore, a different approach to increase the solubility and to induce blue shift of emission color is necessary in order to develop soluble blue TADF emitters.

In this work, two blue TADF emitters, 2,4,6-tri(9H-carbazol-9-yl)-3,5-difluorobezonitrile (3CzFCN) and 2,3,4,6-tetra(9H-carbazol-9-yl)-5-fluorobenzeonitrile (4CzFCN), were developed as soluble blue TADF emitters with improved solubility and blue emission color. The F atom was introduced as an electron withdrawing unit instead of CN to meet the requirements of the soluble blue TADF emitters through improved solubility by hydrophobic nature of F and blue emission by relatively weak electron withdrawing nature of the F atom. The F atom has never been adopted in the molecular design of soluble TADF emitters as well as vacuum evaporable TADF emitters. The two blue TADF emitters exhibited good solubility and could be easily coated by spin-coating process. A high QE of 20.0% with a blue emission color was achieved using the 4CzFCN blue TADF emitter by solution process. This is the first work reporting high QE of 20% in the solution-processed blue TADF OLEDs. It was also demonstrated that the soluble blue TADF OLEDs are comparable to vacuum evaporable blue TADF OLEDs and solution-processed blue phosphorescent OLEDs in terms of QE.

2. Results and Discussion

The soluble blue TADF emitters are required to possess good solubility in solvent, small singlet–triplet energy gap for TADF emission, high photoluminescence (PL) quantum yield, and pure blue emission color. Therefore, electron withdrawing moieties which can increase the solubility of the molecule should be included in the molecular design. We reported that

Dr. Y. J. Cho, Prof. B. D. Chin
Department of Polymer Science and Engineering
Dankook University
152, Jukjeon-ro, Suji-gu, Yongin, Gyeonggi 448-701, Korea
S. K. Jeon, Prof. J. Y. Lee
School of Chemical Engineering
Sungkyunkwan University
2066, Seobu-ro, Jangan-gu, Suwon, Gyeonggi 440-746, Korea
E-mail: leej17@skku.edu

DOI: 10.1002/adfm.201502995

2,4,5,6-tetra(carbazol-9-yl)-1,3-dicyanobenzene (4CzIPN) with two CN units and four carbazole units showed poor solubility in solvent and poor device performances in solution-processed OLEDs in spite of high QE in vacuum-processed OLEDs.[21] The poor solubility of 4CzIPN can be overcome by replacing the highly polar CN unit with hydrophobic F unit which renders the TADF emitter soluble in aromatic solvent. The hydrophobic nature of the F unit may make the TADF emitter compatible with aromatic solvents and facilitate easy penetration of the hydrophobic aromatic solvent for improved solubility compared with H or CN unit. In addition, the weak electron withdrawing character of the F unit compared to the CN unit may shift the emission color to short wavelength. Therefore, the molecular design approach to introduce the F unit would be an effective method to develop soluble blue TADF emitters and highly efficient blue soluble TADF devices.

Two blue TADF emitters with the F functional unit, 3CzFCN and 4CzFCN, were synthesized from 2,3,4,5,6-pentafluorobenzonitrile with five F functional groups. The 2,3,4,5,6-pentafluorobenzonitrile was modified with 9H-carbazole using NaH to prepare the final blue TADF emitters. Both 3CzFCN and 4CzFCN were produced as main products at the same reaction condition because of different reactivity of five F functional groups toward NaH mediated coupling reaction. The F units adjacent to CN unit are more reactive than other F units due to strong electron withdrawing character of the CN unit and are substituted with 9H-carbazole prior to other F units. After that, F unit at 4-position of 2,3,4,5,6-pentafluorobenzonitrile reacts with 9H-carbazole and then the reaction of F units at 3- and 5-positions with 9H-carbazole follows. Therefore, 3CzFCN and 4CzFCN could be simultaneously synthesized from the same 2,3,4,5,6-pentafluorobenzonitrile starting material. The two

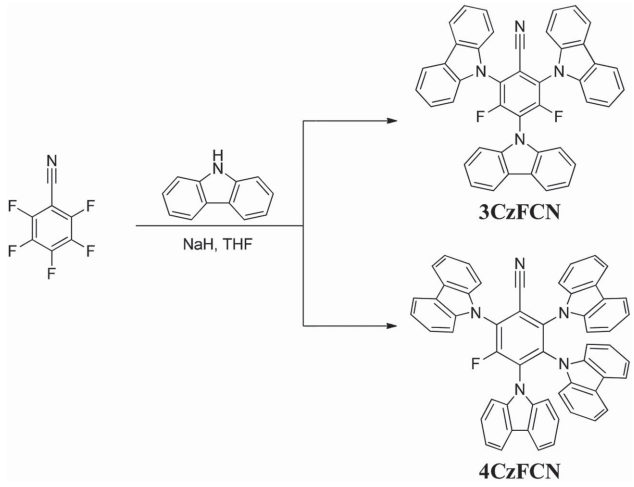

Scheme 1. Synthetic scheme of 3CzFCN and 4CzFCN.

blue TADF emitters were purified by sublimation after isolating the final compounds by column chromatography and were identified by chemical analysis which was described in Experimental Section. **Scheme 1** shows synthetic procedure of the blue emitters and detailed synthetic procedure is also described in Experimental Section.

Feasibility of 3CzFCN and 4CzFCN as TADF emitters was confirmed by electronic molecular orbital distribution calculated using time-dependent density functional theory in **Figure 1**. Gaussian 09 software using B3LYP hybrid functional was used for the calculation. The highest occupied molecular orbital (HOMO) and the lowest unoccupied molecular orbital (LUMO) calculation results were similar in the two TADF

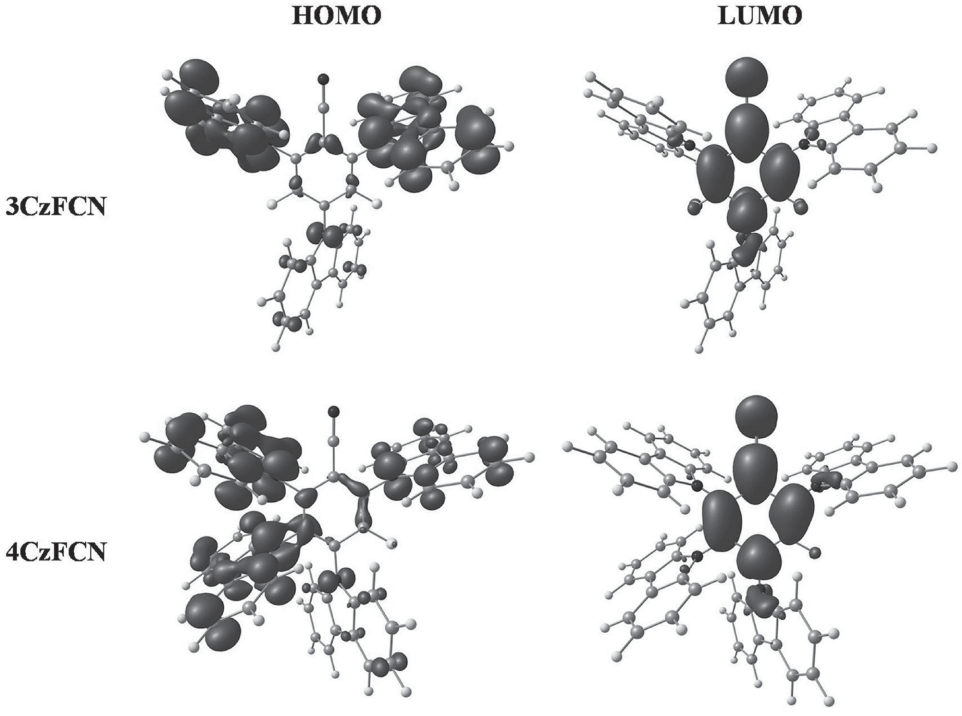

Figure 1. Gaussian simulation images of 3CzFCN and 4CzFCN.

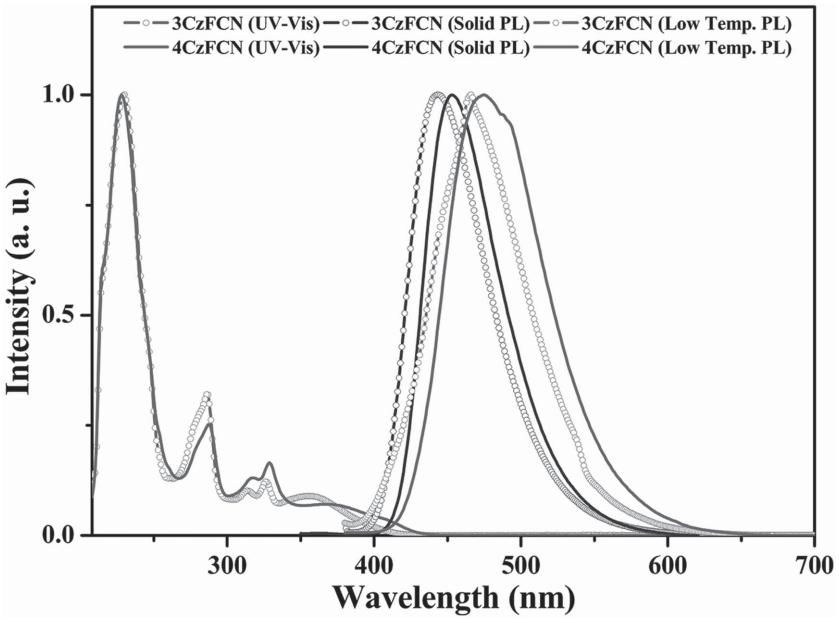

Figure 2. UV–vis absorption and PL spectra of 3CzFCN and 4CzFCN.

emitters. The HOMO and LUMO were largely separated by HOMO dispersion on carbazole and LUMO dispersion on benzonitrile, and were weakly overlapped at the central phenyl ring as observed in the highly efficient TADF emitters.[16] As the HOMO–LUMO separation contributes to small singlet–triplet energy gap (ΔE_{ST}) and the HOMO–LUMO overlap assists high PL quantum yield, both 3CzFCN and 4CzFCN are considered to possess proper HOMO–LUMO distribution for TADF emission. The F functional group had weak influence on the HOMO–LUMO distribution because the LUMO was localized on the benzonitrile unit.

The molecular orbital distribution is reflected in the photophysical performances of TADF emitters obtained using ultraviolet–visible (UV–vis) and PL analysis in **Figure 2**. The UV–vis absorption spectra of 3CzFCN and 4CzFCN were similar because main absorption was induced by carbazole modified benzonitrile backbone structure. However, weak UV–vis absorption at long wavelength was different because the weak absorption was caused by electron transfer absorption from carbazole to benzonitrile which depended on donor and acceptor strength. More carbazole units in 4CzFCN than in 3CzFCN strengthened the donor character, which lead to long wavelength shift of the weak absorption peak. PL emission peak of 4CzFCN was also shifted to long wavelength compared with that of 3CzFCN. 3CzFCN and 4CzFCN exhibited blue PL emission peaks at 443 and 453 nm, respectively. The PL emission peak of 4CzFCN was also shifted to short wavelength compared to that of 4CzIPN. The weaker electron withdrawing character of the F unit than that of CN unit lead to the blue shift of the PL emission wavelength. Singlet energy/triplet energy of 3CzFCN and 4CzFCN were 3.06/3.00 and 2.97/2.91 eV, respectively. Small ΔE_{ST} value of 0.06 eV was obtained in the 3CzFCN and 4CzFCN TADF emitters.

PL quantum yields of 3CzFCN and 4CzFCN were 0.13 and 0.16 in toluene solution without nitrogen bubbling, but they were increased to 0.76 and 0.81 in toluene solution with nitrogen bubbling, indicating that triplet excited state was largely involved in the radiative singlet transition process.[22] PL quantum yields of 3CzFCN and 4CzFCN doped SiCz films were also characterized, which demonstrated that both fluorescent and delayed fluorescent components contributed total PL quantum yield. PL quantum yield of 4CzFCN (1.00) was higher than that of 3CzFCN (0.74), which implies that more carbazole units are favorable for efficient PL emission. PL data are summarized in **Table 1**.

TADF character of 3CzFCN and 4CzFCN was verified by further investigating temperature-dependent transient PL decay in **Figure 3**. The temperature-dependent PL data clearly showed increased delayed PL intensity at high temperature and sharp rise of the delayed PL intensity at a certain temperature (at 200 K in this work). Therefore, 3CzFCN and 4CzFCN can be considered to behave as TADF emitters which utilize triplet excitons for singlet emission. Curve fitting of the PL decay data gave excited state lifetime of delayed PL emission of 28 and 17 μs in 3CzFCN and 4CzFCN, respectively.

The HOMO/LUMO levels were extracted from positive and negative cyclic voltammetry scans in **Figure 4**, and they were −6.38/−3.56 eV and −6.31/−3.49 eV for 3CzFCN and 4CzFCN, respectively. Both deepened HOMO and LUMO was observed

Table 1. A summary of photophysical properties and thermal characteristics of 3CzFCN and 4CzFCN.

Emitter	Absorption coefficient[a] [M^{-1} cm^{-1}]	Φ_{PL}[b] (prompt/total)	τ[c] [μs]	E_S/E_T [eV]	ΔE_{ST} [eV]	T_g[d] [°C]	T_d[e] [°C]
3CzFCN	278 896	0.13/0.76 (solution)	28	3.06/3.00	0.06	134	371
		0.34/0.74 (film)					
4CzFCN	228 307	0.16/0.81 (solution)	17	2.97/2.91	0.06	179	398
		0.57/1.00 (film)					

[a]Measured in 10×10^{-6} M tetrahydrofuran solution; [b]Absolute photoluminance quantum yield evaluated using an integrating sphere in 10×10^{-6} M toluene solution and 10 wt% emitter doped SiCz film without degassing (prompt) and under nitrogen (total); [c]Excited state lifetime of delayed emission at 297 K; [d]Glass transition temperature; [e]Thermal decomposition temperature at 5% weight loss.

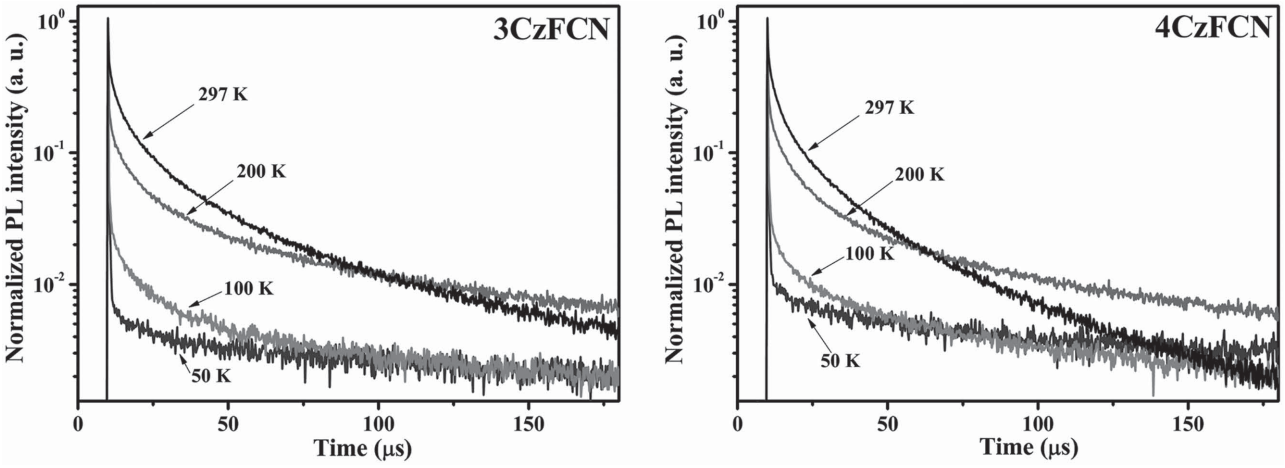

Figure 3. Transient PL decay curves of solution coated SiCz:3CzFCN and SiCz:4CzFCN films at 50, 100, 200, and 297 K.

in the 3CzFCN TADF emitter by less electron donating carbazole units and more electron withdrawing F units than 4CzFCN TADF emitter. The number of electron donors and acceptors could manage the HOMO and LUMO levels of the TADF emitters.

As the main objective of designing and synthesizing 3CzFCN and 4CzFCN was to develop highly soluble blue TADF emitters for solution-processed TADF devices, solubility and film formation of the TADF emitters were studied using atomic force microscope (AFM). 4CzIPN which has similar molecular structure to 4CzFCN could not be coated as a pure film from toluene due to poor solubility. However, 3CzFCN and 4CzFCN could be easily spin-coated from toluene solution at a surface roughness below 0.55 nm. The good solubility of 3CzFCN and 4CzFCN enabled the smooth film–coating from toluene solution as can be proven by AFM data in **Figure 5**. Solubility of 3CzFCN and 4CzFCN in toluene was 1.5 and 1.0 wt%, respectively, which was much higher than that of 4CzIPN (0.1 wt%) in toluene.[21] As explained in the molecular design, the F functional unit had hydrophobic nature rather than hydrophilic nature of CN functional unit, which assisted solubilizing 3CzFCN and 4CzFCN in toluene. The F atom is also advantageous compared with H atom for facile penetration of aromatic solvents for better solubility. The order of solubility of TADF emitters (3CzFCN > 4CzFCN > 4CzIPN) coincided with the number of F units in the molecular structure.

Another important material parameter for solution process application is glass transition temperature (T_g) because low T_g material can be crystallized during annealing process. 3CzFCN and 4CzFCN displayed high T_g of 134 and 179 °C, respectively, as can be identified in heating differential scanning calorimeter thermograms of 3CzFCN and 4CzFCN (**Figure 6**). Decomposition temperatures of 3CzFCN and 4CzFCN were also analyzed by thermogravimetric analysis (TGA). TGA measurements were performed at a heating rate of 10 °C min^{-1}. Decomposition temperatures of 3CzFCN and 4CzFCN at a weight loss of 5% were 371 and 398 °C, respectively (Figure S1, Supporting Information). Therefore, the two TADF emitters are appropriate as the dopant materials for solution process.

Blue PL emission, TADF behavior, good solubility, smooth film morphology, and high T_g of 3CzFCN and 4CzFCN allowed the fabrication of soluble TADF devices by spin-coating process from toluene solution. Host material of the TADF emitters was diphenyldi(4-(9-carbazolyl)phenyl)silane (SiCz) because of smooth film formation[21] and good overlap of PL emission of SiCz with UV–vis absorption of the TADF emitters (Figure S2,

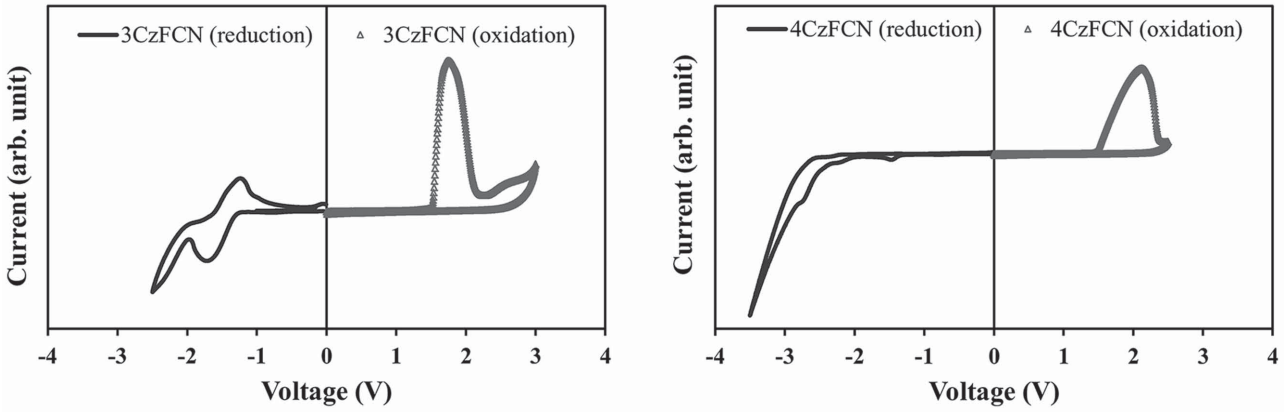

Figure 4. Cyclic voltammetry curves of 3CzFCN and 4CzFCN.

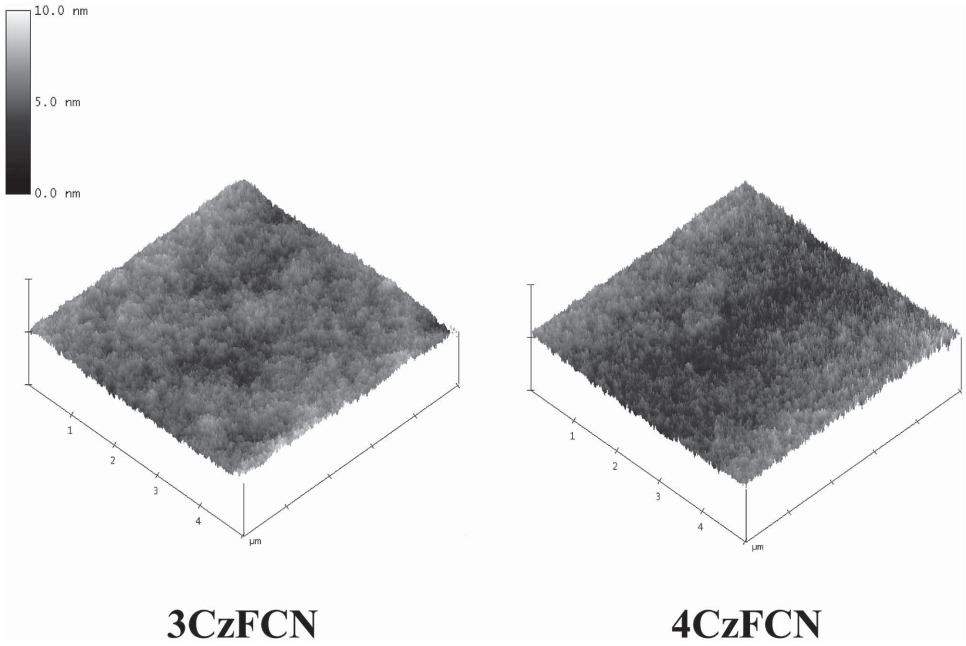

Figure 5. AFM images of spin-coated 3CzFCN and 4CzFCN films.

Supporting Information). Doping concentration of each material was optimized and optimized device data were compared. Optimized doping concentrations of 3CzFCN and 4CzFCN devices were 10% and 15%, respectively, in the SiCz host. Current density–voltage data and luminance–voltage data of the solution-processed TADF devices were added in **Figure 7**. The current density and luminance of the SiCz:4CzFCN device were higher than those of the SiCz:4CzFCN device because of high optimized doping concentration of the TADF emitters which facilitated carrier hopping via dopant materials. QE plots according to current density of the soluble TADF devices are in **Figure 8**. The QE of the SiCz:4CzFCN device was higher than that of the SiCz:3CzFCN device. Maximum QE of the SiCz:4CzFCN device was 20.0%, which is the best QE reported in the solution-processed TADF OLEDs considering that the best QE of the solution-processed green TADF OLEDs is only 18.3% in our previous work.[21] Several factors can explain the high QE of the SiCz:4CzFCN device. First key factor is high PL quantum yield assisted by TADF emission in the radiative transition process. PL quantum yield of 4CzFCN doped in the SiCz host was 1.00 under nitrogen relative to 0.57 in ambient condition. This indicates that all triplet excitons were converted into singlet excitons by up-conversion process, which contributed to the high QE of the SiCz:4CzFCN device. Second factor is good solubility and film-forming capability of 4CzFCN. Smooth film generation without any crystallization during film drying process is essential in the solution process, which was observed in the 4CzFCN emitter due to solubility boosting effect by

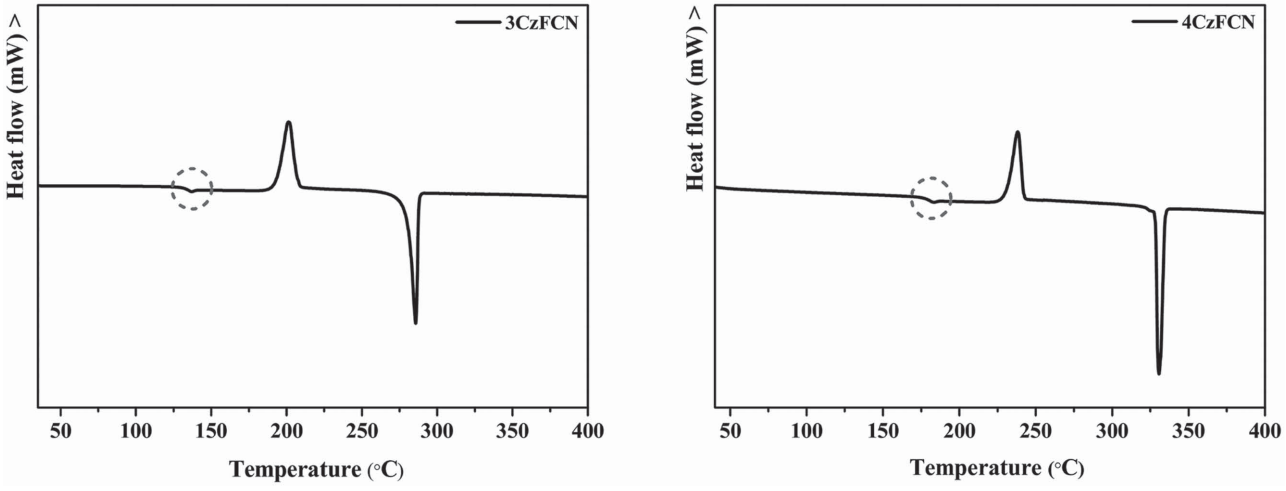

Figure 6. Differential scanning calorimeter thermograms of 3CzFCN and 4CzFCN.

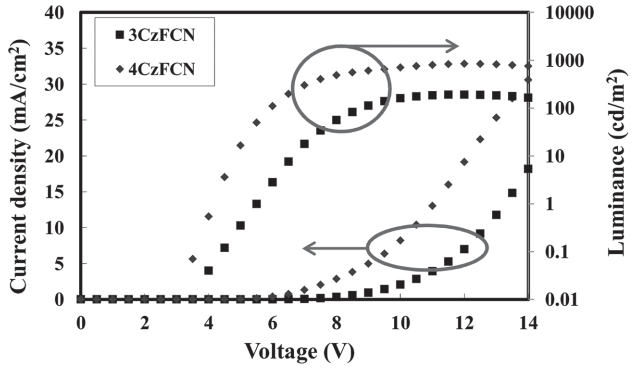

Figure 7. Current density–voltage–luminance curves of solution-processed 3CzFCN and 4CzFCN devices.

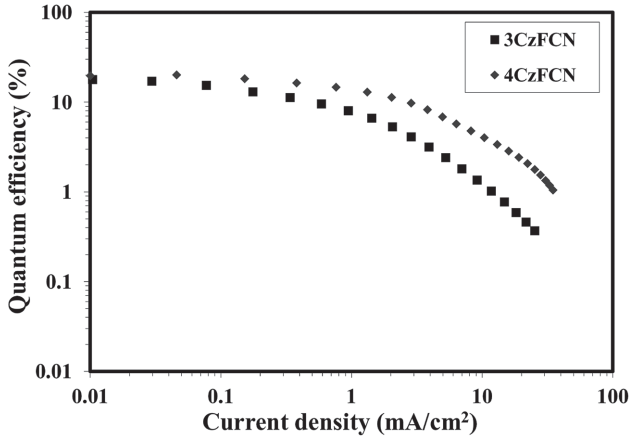

Figure 8. Quantum efficiency–current density curves of soluble 3CzFCN and 4CzFCN TADF devices.

hydrophobic nature of the F functional unit, high T_g, and sterically hindered molecular structure. In addition, short excited state lifetime for delayed PL emission of 4CzFCN contributed to improve the QE at high luminance and alleviate efficiency roll-off problem of the solution-processed devices. In the case of 3CzFCN device, the long excited state lifetime of 3CzFCN caused the serious efficiency roll-off at high luminance. Both SiCz:3CzFCN and SiCz:4CzFCN devices showed high QE as can be confirmed by device data in **Table 2**. Although the QE of the SiCz:3CzFCN device was inferior to that of the SiCz:4CzFCN device, it is a high QE as a QE of deep blue solution-processed

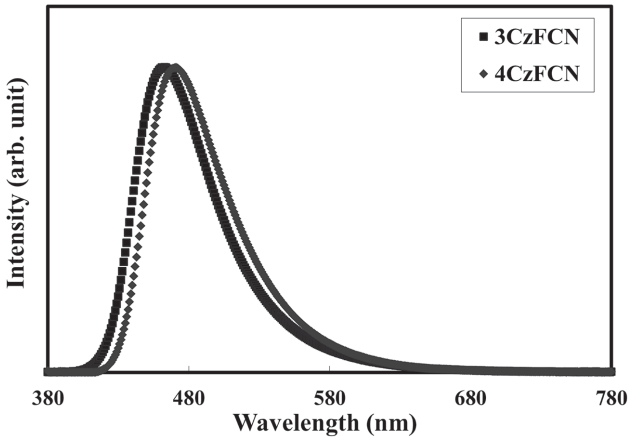

Figure 9. Electroluminescence spectra of soluble 3CzFCN and 4CzFCN TADF devices.

TADF device. Additionally, the QE of the soluble TADF OLEDs fabricated using 4CzFCN dopant is comparable to that of solution-processed blue phosphorescent OLEDs.[13–15] It is even similar to that of vacuum-processed blue TADF OLEDs.[18–20] Furthermore, the QE of the solution-processed 3CzFCN and 4CzFCN devices was even better than that of vacuum-processed 3CzFCN and 4CzFCN devices. To confirm the superiority of the 3CzFCN and 4CzFCN emitter as soluble blue emitters, a well-known blue TADF emitter, 4,5-di(9H-carbazol-9-yl)phthalonitrile (2CzPN), was used to fabricate a standard device. 2CzPN was well dissolved in toluene due to low molecular weight. However, the maximum QE of the solution-processed 2CzPN device was only 5.3%. All device performances of the solution-processed 2CzPN device are shown in Table 2. There, the F introduced molecular design of 3CzFCN and 4CzFCN is superior to the molecular design of 4CzIPN or 2CzPN for blue emission and good solution processibility.

Emission spectra of SiCz:3CzFCN and SiCz:4CzFCN devices are presented in **Figure 9**. The relative peak position of the electroluminescence (EL) spectra of the SiCz:3CzFCN and SiCz:4CzFCN devices was similar to that of PL spectra of SiCz:3CzFCN and SiCz:4CzFCN films in Figure S2 (Supporting Information). Peak positions of EL spectra of SiCz:3CzFCN and SiCz:4CzFCN devices were 463 and 471 nm, respectively. Red shift of the EL wavelength by 8 nm was detected in the SiCz:4CzFCN device. Color coordinates of the SiCz:3CzFCN and SiCz:4CzFCN devices were (0.16,0.19) and (0.16,0.25), respectively.

Table 2. A summary of TADF device performances of 3CzFCN, 4CzFCN, and 2CzPN.

Emitter	Process	CIE (x,y)[a)]	Maximum EQE [%]	Maximum CE [Cd A^{-1}]	EQE[b)] [%]	CE[c)] [Cd A^{-1}]
3CzFCN	Solution	0.16, 0.19	17.8	26.9	8.0	11.8
	Vacuum	016, 0.18	12.9	19.1	10.9	15.8
4CzFCN	Solution	0.16, 0.25	20.0	36.1	16.3	28.8
	Vacuum	0.18, 0.34	17.3	38.0	12.3	26.7
2CzPN	Solution	0.17, 0.27	5.3	10.4	3.8	7.10

[a)]Data of CIE 1931 color space measured at 100 cd m^{-2}; [b)]Data of external quantum efficiency (EQE) measured at 100 cd m^{-2}; [c)]Data of current efficiency (CE) measured at 100 cd m^{-2}.

3. Conclusions

In conclusion, highly efficient solution-processed blue TADF OLEDs could be demonstrated by synthesizing TADF emitters with electron withdrawing and hydrophobic F functional unit to shift EL emission to short wavelength and solubilize the emitters. The introduction of F functional unit as an electron accepting moiety of the TADF emitters was effective to realize blue emission color, high QE, and good processibility. Therefore, the strategy of adopting F functional unit can help to design soluble TADF materials for ink-jet or other printing processes.

4. Experimental Section

General Information: 9H-carbazole was purchased from Aldrich Chem. Co. and tetrahydrofuran (THF); magnesium sulfate and dimethylformamide were purchased from Duksan Sci. Co. Sodium hydride and 2,3,4,5,6-pentafluorobenzonitrile were purchased from Tokyo Chemical Industry Co. These chemicals were used as received. Characterization method used in this work was described in previous paper.[21]

Synthesis: 3CzFCN and 4CzFCN: Sodium hydride (60% in paraffin, 0.73 g, 18.00 mmol) was washed with hexane three times. A solution of 9H-carbazole (2.60 g, 15.50 mmol) in anhydrous THF was poured into dispersion of purified sodium hydride in dry THF at room temperature. After stirring for 30 min, 2,3,4,5,6-pentafluorobenzonitrile (0.50 g, 2.58 mmol) dissolved in anhydrous THF (20 mL) was added to the mixed solution of sodium hydride and 9H-carbazole under a nitrogen atmosphere. The reaction solution was allowed to stir at room temperature overnight. After overnight stirring, the reaction mixture was extracted with dichloromethane and distilled water, and then dried with anhydrous magnesium sulfate. The reaction products of 3CzFCN (R_f: 0.60) and 4CzFCN (R_f: 0.40) were purified by silica gel chromatography using a mixture of chloroform and *n*-hexane as an eluent. Greenish yellow (3CzFCN) and yellow (4CzFCN) powdery products were obtained in 0.80 g and 1.30 g, respectively.

3CzFCN—^{1}H NMR (400 MH_Z, $CDCl_3$): δ 8.17 (d, 4H, J = 7.60 H_Z), 8.13 (d, 2H, J = 8.00 H_Z), 7.58–7.48 (m, 6H), 7.42–7.35 (m, 10H), 7.29–7.27 (m, 2H) ^{13}C NMR (100 MH_Z, $CDCl_3$): δ 140.07, 139.25, 127.13, 126.77, 124.57, 124.45, 121.94, 121.80, 121.02, 120.78, 109.91, 109.32, MS (FAB) *miz* 635 [(M+H)$^+$].

4CzFCN—^{1}H NMR (400 MH_Z, $CDCl_3$): δ 8.20 (d, 2H, J = 7.60 H_Z), 7.73–7.59 (m, 8H), 7.43 (t, 2H, J = 7.80 H_Z), 7.34 (d, 2H, J = 7.60 H_Z), 7.24–7.04 (m, 12H), 6.94 (d, 2H, J = 8.40 H_Z), 6.80 (t, 2H, J = 7.60 H_Z), 6.65 (t, 2H, J = 8.40 H_Z) ^{13}C NMR (100 MH_Z, $CDCl_3$): δ 140.08, 138.76, 138.50, 137.42, 126.76, 125.71, 125.57, 124.69, 124.60, 124.20, 124.10, 123.77, 121.83, 121.32, 121.20, 121.05, 120.74, 120.30, 120.16, 119.55, 109.95, 109.76, 109.71, 109.66, MS (FAB) *miz* 782 [(M+H)$^+$].

Device Fabrication: Solution-processed TADF OLEDs were grown on cleaned indium tin oxide substrate by spin-coating of 60 nm thick poly(3,4-ethylenedioxythiophene)–poly(styrenesulfonate), 15 nm thick poly(9-vinylcarbazole), and 25 nm thick emitting layer having SiCz:3CzFCN or SiCz:4CzFPN. Optimized doping concentration of 10% and 15% was used in the SiCz:3CzFCN and SiCz:4CzFCN emitting layer. Vacuum evaporation process was used for film deposition of 5 nm thick diphenyl(4-(triphenylsilyl)phenyl)phosphine oxide, 30 nm thick 1,3,5-tris(*N*-phenylbenzimidazole-2-yl)benzene, 1 nm thick LiF, and 200 nm thick Al on the spin-coated emitting layer. Other device fabrication procedure and device characterization method were the same as those described in previous work.[21]

Supporting Information

Supporting Information is available from the Wiley Online Library or from the author.

Acknowledgements

This research was supported by Basic Science Research Research Program through the National Research Foundation of Korea (NRF) funded by Ministry of Science, ICT, and future Planning (2013R1A2A2A01067447).

Received: July 19, 2015
Revised: September 5, 2015
Published online: October 15, 2015

[1] J. H. Burroughes, D. D. C. Bradley, A. R. Brown, R. N. Marks, K. Mackay, R. H. Friend, P. L. Burns, A. B. Holmes, *Nature* **1990**, *347*, 539.
[2] G. Gustafsson, Y. Cao, G. M. Treacy, F. Klavetter, N. Colaneri, A. J. Heeger, *Nature* **1992**, *357*, 477.
[3] K. S. Yook, J. Y. Lee, *Adv. Mater.* **2014**, *26*, 4218.
[4] L. Duan, L. Hou, T. Lee, J. Qiao, D. Zhang, G. Dong, L. Wang, Y. Qiu, *J. Mater. Chem.* **2010**, *20*, 6392.
[5] E. Ahmed, T. Earmme, S. A. Jenekhe, *Adv. Funct. Mater.* **2011**, *21*, 3889.
[6] C. W. Lee, J. Y. Lee, *Adv. Mater.* **2013**, *25*, 596.
[7] Y. Tao, Q. Wang, C. Yang, K. Zhang, Q. Wang, T. Zou, J. Qin, D. Ma, *J. Mater. Chem.* **2008**, *18*, 4091.
[8] C.-L. Ho, W.-Y. Wong, G.-J. Zhou, B. Yao, Z. Xie, L. Wang, *Adv. Funct. Mater.* **2007**, *17*, 2925.
[9] L. Hou, L. Duan, J. Qiao, D. Zhang, G. Dong, L. Wang, Y. Qiu, *Org. Electron.* **2010**, *11*, 1344.
[10] Q. Fu, J. Chen, C. Shi, D. Ma, *ACS Appl. Mater. Interfaces* **2012**, *4*, 6579.
[11] K. S. Yook, J. Y. Lee, *J. Mater. Chem.* **2012**, *22*, 14546.
[12] S. A. Choulis, V.-E. Choong, M. K. Mathai, F. So, *Appl. Phys. Lett.* **2005**, *87*, 113503.
[13] J.-H. Jou, W.-B. Wang, S.-Z. Chen, J.-J. Shyue, M.-F. Hsu, C.-W. Lin, S.-M. Shen, C.-J. Wang, C.-P. Liu, C.-T. Chen, M.-F. Wud, S.-W. Liu, *J. Mater. Chem.* **2010**, *20*, 8411.
[14] K. S. Yook, J. Y. Lee, *Org. Electron.* **2011**, *12*, 1711.
[15] C. W. Lee, K. S. Yook, J. Y. Lee, *Org. Electron.* **2013**, *14*, 1009.
[16] H. Uoyama, K. Goushi, K. Shizu, H. Nomura, C. Adachi, *Nature* **2012**, *492*, 236.
[17] F. B. Dias, K. N. Bourdakos, V. Jankus, K. C. Moss, K. T. Karntekar, V. Bhalla, J. Santos, M. R. Bryce, A. P. Monkman, *Adv. Mater.* **2013**, *25*, 3707.
[18] S. Hirata, Y. Sakai, K. Masui, H. Tanaka, S. Y. Lee, H. Nomura, N. Nakamura, M. Yasumatsu, H. Nakatoni, Q. Zhang, K. Shizu, H. Miyazaki, C. Adachi, *Nat. Mater.* **2015**, *14*, 330.
[19] Q. Zhang, B. Li, S. Huang, H. Nomura, H. Tanaka, C. Adachi, *Nat. Photonics* **2014**, *8*, 326.
[20] M. Kim, S. K. Jeon, S.-H. Hwang, J. Y. Lee, *Adv. Mater.* **2015**, *27*, 2515.
[21] Y. J. Cho, K. S. Yook, J. Y. Lee, *Adv. Mater.* **2014**, *26*, 6642.
[22] S. Y. Lee, T. Yasuda, Y. S. Yang, Q. Zhang, C. Adachi, *Angew. Chem.* **2014**, *126*, 6520.